Vibrational Spectroscopy, 3 (1992) 105–113
Elsevier Science Publishers B.V., Amsterdam

Vibrational spectroscopic studies of L,D-alternating valine peptides

Vaman M. Naik

Department of Natural Sciences, University of Michigan–Dearborn, Dearborn, MI 48128 (USA)

(Received 31st May 1991)

Abstract

Raman and infrared spectra of Boc-(L-Val-D-Val)$_n$-OMe [(LD-Val)$_n$], with $n = 4$, 6 and 8, were obtained in crystalline and solution states. Based on predictions from normal-mode calculations of a number of relevant single- and double-stranded β-helix conformations, structures were assigned for the three oligopeptides under the above-mentioned conditions. In the crystalline state, all three oligopeptides have a double-stranded $\uparrow\downarrow\beta^{5.6}$ structure. In cyclohexane and in chloroform, the $\uparrow\downarrow\beta^{5.6}$ structure predominates for (LD-Val)$_4$. In chloroform the (LD-Val)$_6$ has a $\beta^{4.4}$ structure. (LD-Val)$_8$ in cyclohexane and in chloroform exists predominantly in a $\uparrow\downarrow\beta^{5.6}$ structure together with some $\beta^{4.4}$.

Keywords: Infrared spectrometry; Raman spectrometry; Peptides; Valine

During the past few years, peptides and polypeptides with a regular sequence of enantiomeric residues (L and D) along the chain have received considerable attention [1–11]. This is mainly due to their analogy with gramicidin A, a naturally occuring linear pentadecapeptide that forms an ion-conducting channel across natural and synthetic lipid bilayer membranes (for a review, see [12]). These L,D-alternating oligopeptides can assume, in addition to the well known structures such as an α-helical structure, a wide variety of conformations including single (β^n) and double-stranded helices. With double-stranded helices, the conformations could be of parallel ($\uparrow\uparrow\beta^n$) or antiparallel ($\uparrow\downarrow\beta^n$) type. Here, the superscript n refers to the total number of residues per turn of the helix. Two octapeptides, Boc-(L-Val-D-Val)$_4$-OMe and Boc-(L-Phe-D-Phe)$_4$-OMe, are shown to exist in a double-stranded antiparallel β-structure of the type $\uparrow\downarrow\beta^{5.6}$, by single-crystal x-ray diffraction studies [2,3]. The valine octapeptide is shown to be a left-handed whereas the phenylalanine octapeptide is a right-handed helix.

Vibrational spectroscopy (infrared and Raman), through the use of normal-mode analysis to predict the vibrational frequencies expected for a given conformation, can be used to obtain information on the secondary structure of polypeptide molecules [13]. Naik and Krimm [14] have calculated normal modes for several single- ($\beta^{4.4}$ and $\beta^{6.3}$) and double-helical ($\uparrow\downarrow\beta^{5.6}$, $\uparrow\downarrow\beta^{7.2}$, $\uparrow\uparrow\beta^{5.6}$ and $\uparrow\uparrow\beta^{7.2}$) structures and used the results to predict the conformation of gramicidin A in the ion-free crystalline state, ion-bound crystalline state, solution and in synthetic membranes [15,16]. The structures predicted based on vibrational spectroscopy and normal-mode analysis were confirmed later by single-crystal x-ray analyses [17–19]. In the crystalline state, the uncomplexed gramicidin A has a double-stranded $\uparrow\downarrow\beta^{5.6}$ structure [19], whereas a cesium ion com-

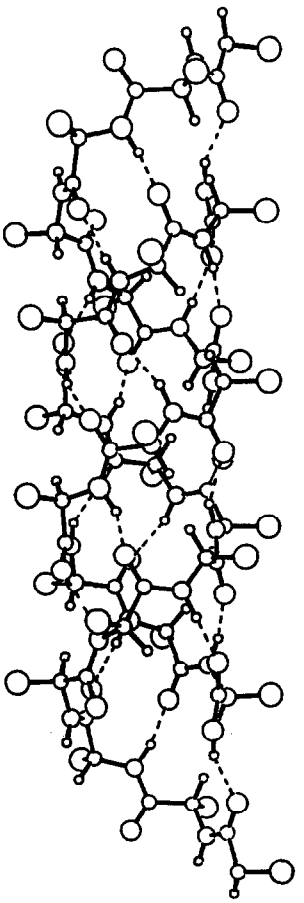

Fig. 1. ORTEP drawing of $\uparrow\downarrow\beta^{5,6}$ structure.

plex adopts a $\uparrow\downarrow\beta^{6,4}$ structure [18]. In lipid vesicles, i.e., in the conducting state, gramidicin A is found in a single-stranded $\beta^{6,3}$ helix [14].

In this work, a series of three valine oligopeptides, namely Boc-(L-Val-D-Val)$_n$-OMe, with n = 4, 6 and 8, were studied; Boc-(L-Val-D-Val)$_n$-OMe is subsequently referred to as (LD-Val)$_n$. The structure of (LD-Val)$_4$ is known to be in the left-handed $\uparrow\downarrow\beta^{5,6}$ which is stabilized by fourteen NH $\cdots$ OC hydrogen bonds. The structure can be regarded as a cylinder with an inner diameter of 5.1 Å [2]. An ORTEP drawing of the $\uparrow\downarrow\beta^{5,6}$-helix is given in Fig. 1. A $\uparrow\downarrow\beta^{5,6}$ structure with fifteen amino acid residues (in each chain) would have a maximum length of 31.5 Å [4], which is long enough to span the lipid bilayer. The structures of (LD-Val)$_6$ and (LD-Val)$_8$ have not yet been determined by x-ray analysis. Infrared (IR) and Raman spectra of all of the above oligopeptides are presented and the possible structures in the crystalline and solution states are discussed.

EXPERIMENTAL

The oligopeptides (LD-Val)$_n$ with n = 4, 6 and 8 were synthesized by and kindly provided by Dr. G.P. Lorenzi. (LD-Val)$_4$ and (LD-Val)$_6$ were deuterated with $CHCl_3$–EtOAc solution floating over D_2O. Ethyl acetate contains 2% of H_2O, and the immiscible peptide $CHCl_3$–EtOAc solution floating over D_2O was stirred for about 2 days. The small amount of H_2O present in EtOAc was exchanged to D_2O, and thus leading to the deuteration of the octapeptide. (LD-Val)$_8$ was deuterated from a solution of $CHCl_3$–MeOD. The molecules were not completely deuterated. However, the deuteration achieved was sufficient to identify the deuteration-sensitive modes.

IR spectra of solid samples were recorded in KBr disks using a Perkin-Elmer Model 180 dispersive spectrometer with ca. 2 cm^{-1} resolution at 1800 cm^{-1} and a Bomem DA/3 Fourier transform IR (FT-IR) spectrometer equipped with an HgCdTe detector. The FT-IR spectra were recorded with a resolution of 1 cm^{-1}. The IR spectra of samples in solution were recorded using a CaF_2 cell with a peptide concentration of ca. 0.5%. The solution IR spectra were recorded using the dispersive spectrometer mentioned above.

Raman spectra were recorded, using a Spex 1403 spectrometer equipped with a double monochromator, with an excitation line of 514.5 nm from a Spectra-Physics Model 165 argon ion laser. For solid samples, an incident laser power of ca. 150 mW was focused at the samples, sealed in glass capillaries. The spectral band pass was ca. 2 cm^{-1} at 514.5 nm and the step resolution used was 1 cm^{-1} in all the spectra. For solution samples, the incident laser power of ca. 200 mW was focused at the capillaries containing the sample solutions. The spectral band pass was ca. 3 cm^{-1} at 514.5 nm. Because of the low concentra-

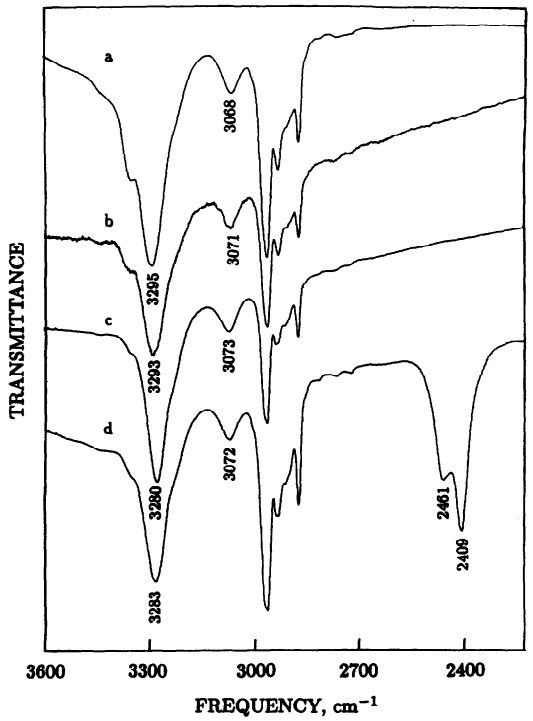

Fig. 2. IR spectra in the 3600–2200 cm^{-1} region of (a) (LD-Val)$_4$, (b) (LD-Val)$_6$, (c) (LD-Val)$_8$ and (d) *N*-deuterated (LD-Val)$_8$.

tion of the samples, the spectra were averaged over a large number of scans (ca. 50) to obtain a better signal-to-noise ratio.

RESULTS

IR spectra of (LD-Val)$_n$ with $n = 4$, 6 and 8 and one of their *N*-deuterated derivatives are shown in Figs. 2–5. The Raman spectra of these molecules are given in Figs. 6 and 7. Figure 8 shows the IR amide I frequencies of (LD-Val)$_6$ and (LD-Val)$_8$ in $CHCl_3$ and Fig. 9 shows the Raman amide I frequencies of all the three valine oligopeptides in $CHCl_3$. Table 1 lists the amide A, B, I, II, III and V frequencies of all three oligopeptides in the crystalline state. Table 2 lists the IR and Raman amide A and amide I frequencies for the three oligopeptides in solution. Table 3 lists the calculated amide I, II, III and V frequencies of the $\uparrow\downarrow\beta^{5.6}$ and $\uparrow\downarrow\beta^{7.2}$ structures [14]. The calculated amide frequencies for the $\beta^{4.4}$ and $\beta^{6.3}$ structures are given in Table 4 [14].

DISCUSSION

Conformation of oligovalines in crystalline state

The vibrations due to CH and CH_3 groups of valine side-chains are very localized and are well characterized [20–22]. The CH_3 group vibrations arising from the oxymethyl and *t*-Boc blocking group, and other end-group frequencies such as the C–O stretching mode, are easily assignable based on the earlier work on ethyl acetate and its *N*-deuterated derivatives [23]. Here mainly the conformationally sensitive modes, namely amide A, B, I, II, III and V modes, will be discussed.

In the conformationally sensitive regions, all three oligopeptides exhibit similar spectra. Amide A and B bands arise from Fermi resonance be-

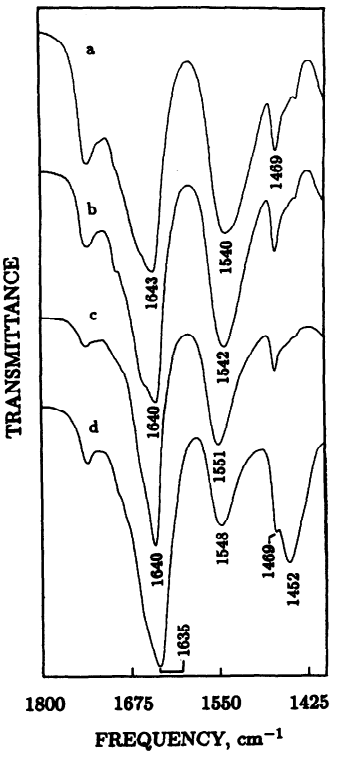

Fig. 3. IR spectra in the 1800–1400 cm^{-1} region of (a) (LD-Val)$_4$, (b) (LD-Val)$_6$, (c) (LD-Val)$_8$ and (d) *N*-deuterated (LD-Val)$_6$.

tween the NH stretching frequency and the first overtone of the amide II (consisting mainly of NH in-plane motion) frequency. Both of these frequencies are sensitive to the backbone conformation of the polypeptide and usually amide A occurs at ca. 3300 cm^{-1} and amide B at ca. 3100 cm^{-1}.

The amide A band observed at 3295 cm^{-1} in both the IR and Raman (R) spectra for (LD-Val)$_4$ shifts down to 3293 cm^{-1} (IR) and to 3290 cm^{-1} (R) in (LD-Val)$_6$, and finally to 3280 cm^{-1} (IR) and to 3267 cm^{-1} (R) in (LD-Val)$_8$. This downward shift of the amide A frequency on going from the octapeptide to the hexadecapeptide indicates that the hydrogen bonds in the latter peptide are stronger than those in the former. The amide B mode is observed in the IR spectrum at 3068 cm^{-1} in (LD-Val)$_4$, at 3071 cm^{-1} in (LD-Val)$_6$ and at 3073 cm^{-1} in (LD-Val)$_8$. The amide B frequency is very weak in the Raman spectrum and frequently is not detectable.

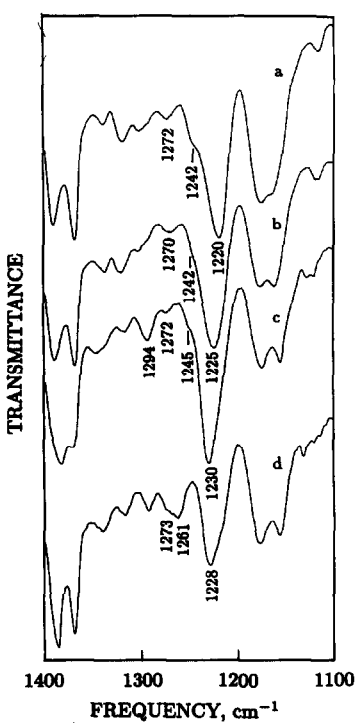

Fig. 4. IR spectra in the 1400–1100 cm^{-1} of (a) (LD-Val)$_4$, (b) (LD-Val)$_6$, (c) (LD-Val)$_8$ and (d) *N*-deuterated (LD-Val)$_8$.

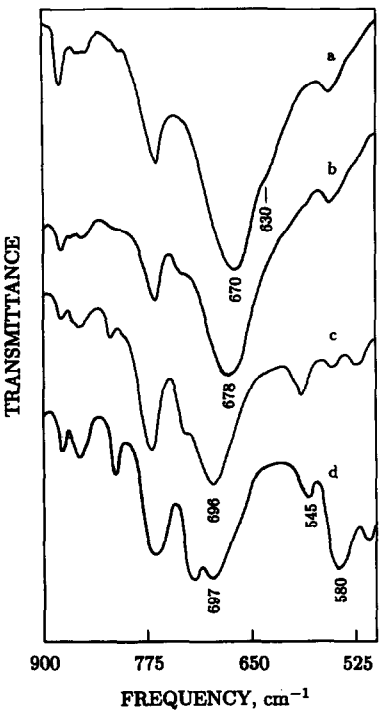

Fig. 5. IR spectra in the 900–500 cm^{-1} region of (a) (LD-Val)$_4$, (b) (LD-Val)$_6$, (c) (LD-Val)$_8$ and (d) *N*-deuterated (LD-Val)$_8$.

The amide I modes essentially consist of CO stretching. The Raman amide I band of (LD-Val)$_4$ has more structure compared with the other two peptides (see Fig. 6). The strongest Raman amide I band is observed at 1678 cm^{-1} for (LD-Val)$_4$, at 1676 cm^{-1} for (LD-Val)$_6$ and at 1672 cm^{-1} for (LD-Val)$_8$. In (LD-Val)$_4$ the shoulder observed at ca. 1665 cm^{-1} in the Raman spectrum becomes a well resolved band at low temperature (77 K). Two more shoulders, at ca. 1693 cm^{-1} and ca. 1650 cm^{-1}, are also visible at this temperature (spectrum not shown). In the IR spectrum, the amide I modes for these peptides are observed at ca. 1643 cm^{-1} for (LD-Val)$_4$ and at 1640 cm^{-1} for (LD-Val)$_6$ and (LD-Val)$_8$. All three peptides show a shoulder near 1685 cm^{-1} in the IR spectrum, a characteristic of an antiparallel β-sheet structure. These small differences observed in the strong amide I frequencies are attributable to the different chain lengths in these three peptides. (LD-Val)$_8$, being the longest, is expected to form a more regular structure than the shorter oligopeptides.

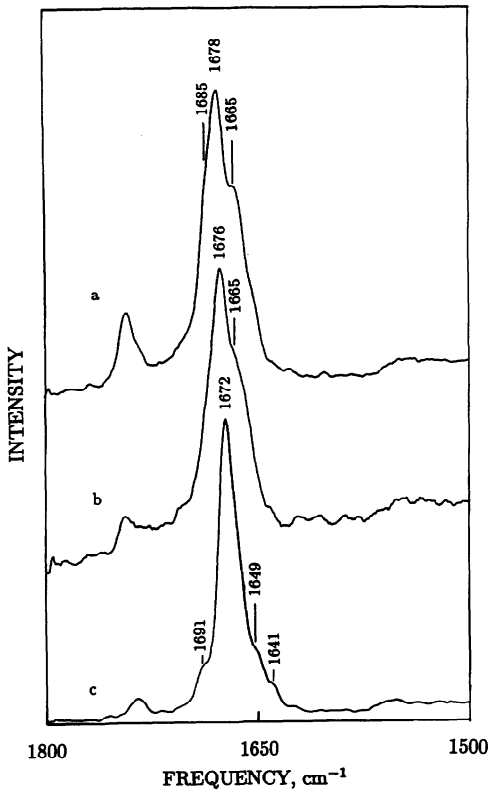

Fig. 6. Raman spectra in the 1800–1500 cm^{-1} region of (a) (LD-Val)$_4$, (b) (LD-Val)$_6$ and (c) (LD-Val)$_8$.

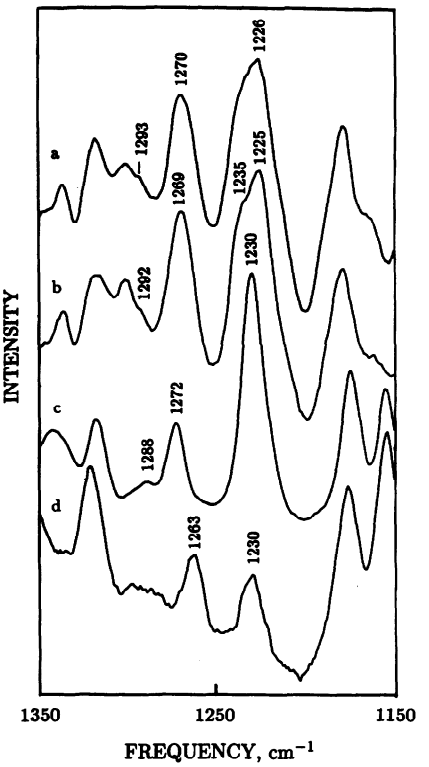

Fig. 7. Raman spectra in the 1350–1150 cm^{-1} of (a) (LD-Val)$_4$, (b) (LD-Val)$_6$, (c) (LD-Val)$_8$ and (d) *N*-deuterated (LD-Val)$_8$.

The calculations of the normal modes of vibrations of the infinite double helices [14] predict a strong (intense) parallel-polarized (parallel to the helix axis) amide I mode in $\uparrow\downarrow\beta^{5.6}$ at 1636 cm^{-1} (see Table 3). The corresponding calculated mode in $\uparrow\downarrow\beta^{7.2}$ is at 1632 cm^{-1}. The strongest IR amide I mode is expected to be an *A* symmetry species mode and parallel-polarized. The calculated frequency of 1636 cm^{-1} is close to those observed for (LD-Val)$_6$ and (LD-Val)$_8$. The strong IR amide I mode observed in (LD-Val)$_4$ is 7 cm^{-1} higher than that predicted for the $\uparrow\downarrow\beta^{5.6}$ structure. The shorter length of (LD-Val)$_4$ compared with the other two peptides can account for this observed difference. As the calculations [14] were done on infinite chains, better agreement is expected with predicted frequencies in longer chains. The lowest amide I mode calculated in $\uparrow\downarrow\beta^{5.6}$ matches very well the strongest observed

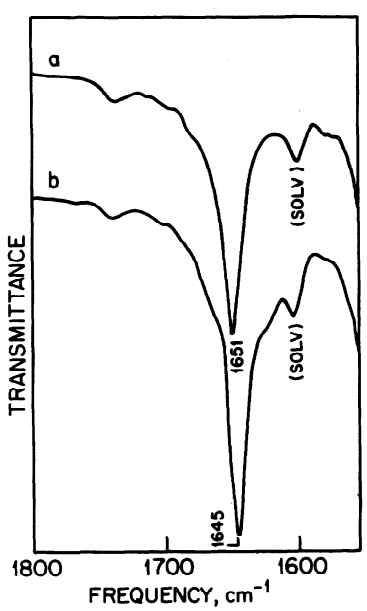

Fig. 8. IR spectra in the 1800–1500 cm^{-1} region of (a) (LD-Val)$_6$ and (b) (LD-Val)$_8$ in chloroform.

TABLE 1

Observed amide frequencies (cm^{-1}) of (LD-Val)$_n$ in the crystalline state [a]

Mode	(LD-Val)$_4$		(LD-Val)$_6$		(LD-Val)$_8$	
	Raman	IR	Raman	IR	Raman	IR
Amide A	3295 w	3295 vs	3290 w	3293 vs	3267 w	3280 vs
Amide B		3068 w		3071 w		3073 w
Amide I	1685 sh	1685 sh		1692 sh	1691 sh	1681 sh
	1678 s		1676 s		1672 vs	
	1665 sh	1660 sh	1665 sh			
	1652 sh		1654 sh	1654sh	1649 sh	1652 sh
		1643 vs		1640 vs	1641 sh	1640 vs
Amide II	1541 vw	1540 s	1542 vw	1542 s	1551 vw	1551 s
Amide III			1292 sh		1288 w	1294 vw
	1270 m	1272 vw	1269 m	1270 w	1272 m	1272 w
	1236 sh	1242 sh	1235 sh	1242 sh		1245 sh
	1226 s	1220 m	1225 s	1225 m	1230 s	1230 m
Amide V	699 vw				694 w	696 m
	670 vw	670 m		678 m	670 vw	
			651 sh			
	627 vw	630 sh	636 w	630 sh		

[a] s = Strong, m = medium, v = very, w = weak and sh = shoulder.

IR mode at 1640 cm^{-1} in (LD-Val)$_6$ and (LD-Val)$_8$. The strong Raman amide I mode observed at 1672 cm^{-1} in these peptides is well reproduced by $\uparrow\downarrow\beta^{5.6}$ and $\uparrow\downarrow\beta^{7.2}$ structures. Hence the calculated frequencies in the amide I region slightly favor the $\uparrow\downarrow\beta^{5.6}$ over the $\uparrow\downarrow\beta^{7.2}$ structure for (LD-Val)$_6$ and (LD-Val)$_8$.

The amide II mode (consisting of mainly NH in-plane motion and CN stretching) is intrinsically weak in the Raman spectrum and is not observed most of the time. It is observed in the IR spectrum usually as a broad, medium strong band at ca. 1550 cm^{-1}. The observed amide II frequencies (see Table 1) are consistent with the predicted frequencies for the $\uparrow\downarrow\beta^{5.6}$ structure (1553–1541 cm^{-1}). However, it should be pointed out that the amide II frequencies are usually not very helpful in discriminating between $\uparrow\downarrow\beta^{5.6}$ and $\uparrow\downarrow\beta^{7.2}$ structures [14,16]. Reliable intensity calculations will be very useful in this regard.

TABLE 2

Observed amide A and I frequencies (cm^{-1}) of (LD-Val)$_n$ in solution

Mode	(LD-Val)$_4$		(LD-Val)$_6$		(LD-Val)$_8$	
	Raman [a]	IR [b]	Raman [a]	IR [a]	Raman [a]	IR [a]
Amide A		3295 s		3290 s		3280 s
Amide I	1695 sh	1691 sh	1689 sh	1680 sh	1684 sh	
	1675 vs	1670 sh	1672 vs		1672 vs	
			1655 sh			
	1644 w	1654 vs	1642 sh	1651 vs		1645 vs

[a] In chloroform solution. [b] In cyclohexane solution; from [24].

In the amide III (generally consisting of NH in-plane motion and CN stretching) region, there are four bands in the IR spectrum, at 1294, 1272, 1245 and 1230 cm^{-1}, in (LD-Val)$_8$ which lose intensity on *N*-deuteration. In the IR spectra the loss of intensity in the 1272 cm^{-1} band is not clearly seen as some other higher frequency band moves into that region after *N*-deuteration. In the Raman spectrum there are three observed amide III bands, at 1288, 1272 and 1230 cm^{-1}. For the $\uparrow\downarrow\beta^{5.6}$ structure, modes with NH in-plane contributions are calculated [14] at 1288, 1284, 1267, 1265 and 1240–1236 cm^{-1}. The observed frequencies for the three oligopeptide are in agreement with the calculated frequencies for the $\uparrow\downarrow\beta^{5.6}$ structure. The $\uparrow\downarrow\beta^{7.2}$ structure does not predict very well the lowest observed amide II band at 1230 cm^{-1} or the higher frequency at 1288 cm^{-1}.

Amide V frequencies (consisting of CN torsional and NH out-of-plane motions) are weak in the Raman spectrum and are fairly intense in the IR spectrum. These are easily detectable by *N*-deuteration. For the $\uparrow\downarrow\beta^{5.6}$ structure, the amide V modes are calculated at 725–707, 695–692, 656 and 640 cm^{-1}. The observed amide V modes for the three oligopeptides (see Table 1) are consistent with the $\uparrow\downarrow\beta^{5.6}$ structure. However, it should be pointed out that the predicted frequencies for the $\uparrow\downarrow\beta^{7.2}$ structure are also comparable to the observed frequencies, but the predicted amide V modes for the parallel double-stranded helices ($\uparrow\uparrow\beta^{5.6}$ and $\uparrow\uparrow\beta^{7.2}$) are clearly inconsistent with the observed frequencies [14].

In summary, the similarity of the observed spectra of (LD-Val)$_n$ with $n = 4$, 6 and 8 indicates that the structures of these peptides in the crys-

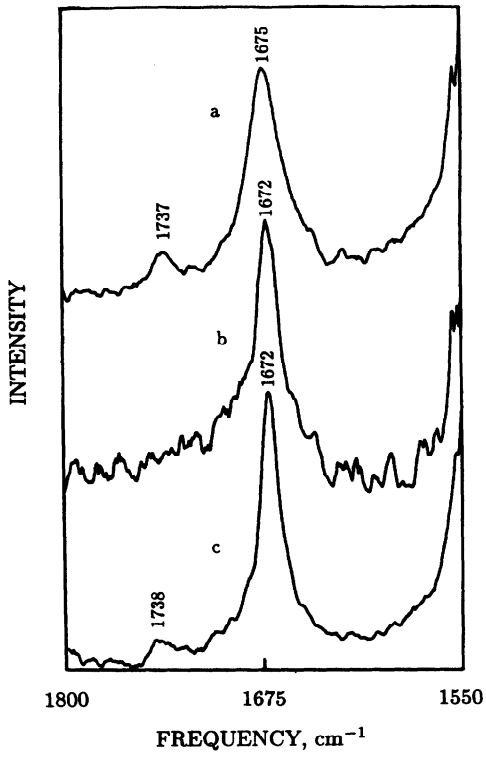

Fig. 9. Raman spectra in the 1800–1550 cm^{-1} region of (a) (LD-Val)$_4$, (b) (LD-Val)$_6$ and (c) (LD-Val)$_8$ in chloroform.

TABLE 3

Calculated amide I, II, III and IV frequencies for $\uparrow\downarrow\beta^{5.6}$ and $\uparrow\downarrow\beta^{7.2}$ structures [a]

Mode	$\uparrow\downarrow\beta^{5.6}$			$\uparrow\downarrow\beta^{7.2}$		
	Species [b]			Species [b]		
	A	E_1	E_2	*A*	E_1	E_2
Amide I	1672	1675	1674	1686	1677	1675
	1669	1669	1674	1674	1674	1674
	1666	1666	1671	1667	1662	1671
	1636 [c]	1656	1662	1632 [c]	1651	1667
Amide II	1547	1553	1547	1556	1556	1559
	1547	1550	1546	1554	1555	1555
	1535	1542	1544	1537	1552	1549
	1531	1541	1543	1537	1549	1547
Amide III	1386	1374	1378	1316	1393	1379
	1385	1373	1377	1314	1392	1378
	1312	1341	1334	1296	1344	1365
	1309	1340	1333	1294	1344	1364
	1288	1267	1271	1246	1274	1266
	1284	1265	1268	1244	1273	1265
	1240	1237	1238		1245	1245
		1236	1236		1244	1244
Amide V	725	720	719	680	684	637
	717	717	716	668	643	631
	714	707	708	658	634	626
	712	695	694	629	627	618
	692	656	637	625	617	
		640		616		

[a] From Naik and Krimm [14]. [b] Modes of *A* and E_1 symmetry are both Raman and IR active whereas modes of E_2 symmetry are only Raman active. [c] Highest intensity IR mode.

TABLE 4

Calculated amide I, II, III and V frequencies for $\beta^{4.4}$ and $\beta^{6.3}$ structures [a]

Mode	$\beta^{4.4}$			$\beta^{6.3}$		
	Species [b]			Species [b]		
	A	E_1	E_2	A	E_1	E_2
Amide I	1648	1653	1681	1652	1654	1652
	1631 [c]	1644	1672	1643 [c]	1645	1652
Amide II	1540	1564	1543	1570	1572	1573
	1534	1538	1538	1542	1559	1557
Amide III	1358	1363	1359	1376	1442	1439
	1327	1330	1328	1321	1401	1406
	1218	1249	1218	1264	1303	1301
	1186	1224	1187	1201	1266	1266
	1181	1179	1181	1182	1207	1208
					1187	1187
Amide V	734	733	735	698	698	696
	683	720	685	677	677	678
		680		574	658	644

[a-c] See Table 3.

talline state are similar. As (LD-Val)$_4$ is known to exist as a $\uparrow\downarrow\beta^{5.6}$ helix in the crystalline state, the fact that the IR and Raman spectra of these three oligopeptides are similar implies a $\uparrow\downarrow\beta^{5.6}$ structure for (LD-Val)$_6$ and (LD-Val)$_8$ in the crystalline state. The amide A, B, I, II, III and V frequencies observed in (LD-Val)$_8$ represent the characteristic of a $\uparrow\downarrow\beta^{5.6}$ structure.

Conformation of oligovalines in solution

For (LD-Val)$_4$ there are no major differences in the observed frequencies, in the amide A and I regions, compared with the solid-state spectra. The strongest Raman band observed at 1678 cm^{-1} in the solid state shifts to 1675 cm^{-1} in $CHCl_3$. The strongest IR band, observed at 1644 cm^{-1} in the solid state, shifts to 1645 cm^{-1} in cyclohexane (spectrum not shown, see [24]). This difference is within the experimental uncertainty in measuring the peak positions. Amide A is observed at 3295 cm^{-1} both in the solid and in cyclohexane. This clearly indicates that the structure of (LD-Val)$_4$ in cyclohexane is essentially similar to its structure in the crystalline state. These results are in agreement with the earlier NMR and IR studies [24]. However, in chloroform it exists as a $\uparrow\downarrow\beta^{5.6}$ and a mixture of various interconverting conformers, as indicated by NMR results [24]. The present Raman spectra do not show any appreciable difference between the two solvents $CHCl_3$ and cyclohexane. This probably means that the percentage of interconverting conformers in $CHCl_3$ is very small compared with $\uparrow\downarrow\beta^{5.6}$ conformers.

For (LD-Val)$_6$, the IR and Raman spectra in chloroform are notably different compared with the solid state. The strongest Raman band observed at 1676 cm^{-1} in the solid shifts down to 1672 cm^{-1} and a new band appears (shoulder) at ca. 1689 cm^{-1}. The strongest IR band observed at 1640 cm^{-1} in the solid shifts up to 1651 cm^{-1} in $CHCl_3$ (see Fig. 8). The higher frequency region of amide I band (ca. 1680 cm^{-1}) in $CHCl_3$ is not as asymmetric as it is in the solid state, there being only a weak shoulder near 1680 cm^{-1}. The large upward shift observed in the amide I mode in $CHCl_3$ indicates a different conformation of the molecule. The 1651 cm^{-1} band may be due to the presence of a $\beta^{4.4}$ single-helical structure in $CHCl_3$ solution. The predicted frequencies for the $\beta^{4.4}$ and $\beta^{6.3}$ structures (see Table 4) are at ca. 1650 cm^{-1} in the A symmetry species [14]. Comparable frequencies are not predicted for the double helical structures (see Table 3). This makes it possible to assign either $\beta^{4.4}$ or $\beta^{6.3}$ structure for (LD-Val)$_6$ in $CHCl_3$ solution. However, the $\beta^{6.3}$ structure can be ruled out based on the predicted Raman active modes. The $\beta^{6.3}$ structure has no calculated frequencies greater than 1654 cm^{-1} whereas $\beta^{4.4}$ has a 1672 cm^{-1} mode in E_2 symmetry species which matches very well the observed Raman band at 1672 cm^{-1}. These results are in agreement with the NMR studies of Tomasic et al. [25]. They showed that the double-stranded helical species $\uparrow\downarrow\beta^{5.6}$ is predominant in fresh solutions of samples obtained from $CHCl_3$–EtOAc. At equilibrium there are three slowly interconverting species. One is the left-handed $\uparrow\downarrow\beta^{5.6}$ species and the other two are most likely single-stranded $\beta^{4.4}$ species of opposite handedness. In the present studies the samples were probably equilibrated because of the long time involved in recording the Raman spectra and the predominant species were single helical structures.

For (LD-Val)$_8$, there are no major differences in the amide A and I modes between the solid state and $CHCl_3$ solution. This behavior is similar to that of (LD-Val)$_4$ discussed above. The strongest Raman amide I band is observed at 1672 cm^{-1} in both the solid state and $CHCl_3$. The strongest IR amide I band shifts from 1640 cm^{-1} in the solid state to 1645 cm^{-1} in $CHCl_3$ solution. The amide A band is observed at 3280 cm^{-1} in both solid and solution states. NMR studies [26] of this peptide in $CHCl_3$ have suggested the presence of $\beta^{4.4}$ helices. The present spectroscopic studies indicate that the conformation is similar to its conformation in the solid state. A 5 cm^{-1} shift in amide I frequency in $CHCl_3$ solution may indicate that there is some conformational change in $CHCl_3$ solution. However, this change is not as large as that observed in (LD-Val)$_6$. However, as the frequency shift is consistent with the predicted modes for the $\beta^{4.4}$ structure, it is possible that there is a mixture of conformers in solution.

Conclusions

From IR and Raman spectroscopic measurements, in conjunction with normal-mode analysis, it has been able to assign the structures for (LD-Val)$_n$ with $n = 4$, 6 and 8 in solid and solution states. The results show that these LD-oligopeptides adopt different structures depending on the environment.

The results show that all three oligopeptides exist in the $\uparrow\downarrow\beta^{5.6}$ structure in the crystalline state. This is the structure in which the uncomplexed gramicidin A exists in the crystalline state. In solution these peptides exist in a mixture of conformations: (LD-Val)$_4$ as $\uparrow\downarrow\beta^{5.6}$ together with some $\beta^{4.4}$, (LD-Val)$_6$ mainly as $\beta^{4.4}$ and (LD-Val)$_8$ mainly as $\uparrow\downarrow\beta^{5.6}$ mixed with some $\beta^{4.4}$. It is interesting that gramicidin A has a $\beta^{6.3}$ structure in liposome suspension in water [16]. However, gramicidin A has not been found with a $\beta^{4.4}$ structure either in the crystalline state or in solution.

The author is grateful to Dr. S. Krimm for providing the use of his spectroscopy laboratory, Dr. G.P. Lorenzi for providing the samples used in this work and Dr. J. Bandekar for useful discussions. The author is indebted to the Horace H. Rackham School of Graduate Studies for faculty fellowship.

REFERENCES

1 D.W. Urry, Proc. Natl. Acad. Sci. U.S.A., 68 (1971) 672.
2 B. Di Blasio, E. Benedetti, V. Povone, C. Pedone and G.P. Lorenzi, Biopolymers, 28 (1989) 193.
3 B. Di Blasio, E. Benedetti, V. Povone, C. Pedone, C. Gerber and G.P. Lorenzi, Biopolymers, 28 (1989) 203.
4 B.V.V. Prasad and R. Chandrasekaran, Int. J. Pept. Protein Res., 10 (1977) 129.
5 W.R. Veatch, E.T. Fossel and E.R. Blout, Biochemistry, 13 (1974) 5249.
6 G.P. Lorenzi, C. Gerber and H. Jäckle, Macromolecules, 18 (1985) 154.
7 G.P. Lorenzi and L. Tomasic, Macromol. Chem., 189 (1988) 207.
8 E. Fenude, L. Tomasic and G.P. Lorenzi, Biopolymers, 28 (1989) 185.
9 F.T. Hesselink and H.A. Scheraga, Macromolecules, 5 (1972) 455.
10 B. Lotz, F. Colonna-Cesari, F. Heitz and G. Spach, J. Mol. Biol., 106 (1976) 915.
11 F. Colonna-Cesari, S. Premilat, F. Heitz, G. Spach and B. Lotz, Macromolecules, 10 (1977) 128.
12 P.C. Jordan, J. Phys. Chem., 91 (1987) 6582.
13 S. Krimm and J. Bandekar, Adv. Protein Chem., 38 (1986) 181.
14 V.M. Naik and S. Krimm, Biophys. J., 49 (1986) 1131.
15 V.M. Naik and S. Krimm, Biochem. Biophys. Res. Commun., 125 (1984) 919.
16 V.M. Naik and S. Krimm, Biophys. J., 49 (1986) 1147.
17 B.A. Wallace, Biophys. J., 49 (1986) 295.
18 B.A. Wallace and K. Ravikumar, Science, 241 (1988) 182.
19 D.A. Langs, Science, 241 (1988) 188.
20 J.L. Koenig and P.L. Sutton, Biopolymers, 10 (1971) 89.
21 L. Simons, G. Bergström, G. Blomfelt, S. Forss, H. Stenbäck and G. Wansen, Commentat. Phys.-Math., Soc. Sci. Fenn., 42 (1972) 125.
22 B.G. Frushour, P.C. Painter and J.L. Koenig, J. Macromol. Sci. Rev. Macromol. Chem., C15 (1976) 29.
23 W.O. George, T.E. Houston and W.C. Harris, Spectrochim. Acta, 30 (1974) 1035.
24 G.P. Lorenzi, H. Jäckle, L. Tomasic, V. Rizzo and C. Pedone, J. Am. Chem. Soc., 104 (1982) 1728.
25 L. Tomasic, A. Stefani and G.P. Lorenzi, Helv. Chim. Acta, 63 (1980) 2000.
26 G.P. Lorenzi, H. Jäckle, L. Tomasic and C. Pedone, Biopolymers, 22 (1983) 157.